Journal of Crystal Growth 637–638 (2024) 127716

Contents lists available at ScienceDirect

Journal of Crystal Growth

journal homepage: www.elsevier.com/locate/jcrysgro

Features of the melt–solution synthesis of the $TbCr_3(BO_3)_4$ single crystals

I.A. Gudim *, N.V. Mikhashenok, A.D. Vasiliev, S.V. Melnikova, M.S. Pavlovskii, S.A. Skorobogatov, A.I. Pankrats

Kirensky Institute of Physics, Krasnoyarsk Scientific Center, Siberian Branch, Russian Academy of Sciences, Krasnoyarsk 660036 Russia

ARTICLE INFO

Communicated by Vincent J. Fratello

Keywords:
A2. Growth from melt-solution
A2.Single crystal growth
B1.Cromium borates
B1. Rare-earth compounds
B1. Oxides
B2. Magnetic materials

ABSTRACT

The phase formation of terbium chromoborate $TbCr_3(BO_3)_4$ in the bismuth trimolybdate and lithium tungstate melt–solutions has been studied. The absence of the terbium chromoborate trigonal phase in the bismuth trimolybdate-based system at all component ratios has been shown. The component ratio in the lithium tungstate-based system has been found at which the $TbCr_3(BO_3)_4$ trigonal crystals are formed at temperatures above 1100 °C; below this temperature, the monoclinic phase dominates. The structural and magnetic properties of the grown crystals have been studied. It has been established that the trigonal and monoclinic $TbCr_3(BO_3)_4$ crystals synthesized from the lithium tungstate-based solvent exhibit identical magnetic properties. At the same time, a significant difference of the magnetic properties of the single crystals synthesized from the bismuth molybdate melt–solution has been observed. This difference has been attributed to the effect of Bi^{3+} ions that partially replace Tb^{3+} ions.

1. Introduction

Recently, there has been a keen interest in crystals with multiferroic properties. The correlation of the characteristics of these materials with their structure and composition has been explored. Among the compounds that exhibit various multiferroic properties is the family of trigonal rare-earth oxyborates with a huntite structure (sp. gr. $R32$ or $P312_1$) [1–3]. This family is interesting for its high variability at both the lanthanide and transition element positions. Initially, these crystals attracted attention as media for self-frequency doubling lasers. Already in the 80 s of the last century, intense research in this area was carried out [4–5]. The nonlinear-optical properties of these materials were found to be no less intriguing [6–8]. Only after some time, their magnetic and piezoelectric properties came into focus.

Ferroborate crystals with a huntite structure have been intensively investigated for more than 20 years [9–11]. Alumo-, gallo-, and scandoborate crystals were studied in significantly fewer works [12–14]. Another understudied subfamily is the chromium compounds with a huntite structure.

We turned to the $TbCr_3(BO_3)_4$ crystals, since only the compounds based on terbium ions (ferro- and alumoborates) exhibit magnetoelectric and magnetooptical properties up to room temperatures, while the compounds containing other rare-earth ions lose these properties at much lower temperatures.

Previously, chromium oxyborate crystals were conventionally grown from melt–solutions based on potassium molybdate K_2MoO_4 and boron oxide [15–18]. However, in [16], it was noted that some of the grown crystals contained up to 10 % of another phase. In addition, the spectroscopy study of the ytterbium-doped yttrium alumoborate single crystals grown from different melt–solution systems revealed a fairly large amount of potassium and molybdenum impurities when a potassium-molybdate system was used in the growth [19]. In addition, it was shown that the impurity content in the crystals grown from the bismuth-molybdate melt–solution was noticeably lower. Therefore, the first system tried by us for growing terbium chromoborate single crystals was the bismuth-molybdate one.

2. Crystallization from the bismuth-molybdate melt–solution

Taking into consideration our experience in growing alumo- and ferroborates with a huntite structure, we selected a solvent with a bismuth trimolybdate to boron oxide molar ratio of $Bi_2Mo_3O_{12}$: B_2O_3 = 1: 2. This solvent was added with the crystal-forming oxides in stoichiometric concentrations (10 wt%). The saturation temperature T_{sat} of the prepared melt–solution turned out to be higher than 1200 °C. However, down to T = 800 °C, the only crystallizing phase was chromium oxide. As a result of a gradual increase in the boron oxide content in the solvent, chromium borate $CrBO_3$ became the crystallizing phase at a ratio

* Corresponding author.
E-mail address: irinagudim@mail.ru (I.A. Gudim).

https://doi.org/10.1016/j.jcrysgro.2024.127716
Received 14 February 2024; Received in revised form 16 April 2024; Accepted 17 April 2024
Available online 18 April 2024

of $Bi_2Mo_3O_{12}$: B_2O_3 = 1: 3. The next stage was the introduction of superstoichiometric terbium oxide Tb_2O_3. After the terbium oxide to bismuth trimolybdate molar ratio attained 0.3: 1, the crystallizing phase changed again: $TbCr_3(BO_3)_4$ appeared, but, unfortunately, with only monoclinic symmetry (sp. gr. *C2/c*). Further changes in the melt–solution did not lead to the appearance of the trigonal phase. The final quasi-binary form of the melt–solution can be written as

$$92\ \text{wt}\ \%\ \{Bi_2Mo_3O_{12} + 3B_2O_3 + 0.3Tb_2O_3\} + 8\ \text{wt}\%\ TbCr_3(BO_3)_4 \quad (1)$$

To study the physical properties of monoclinic terbium chromoborate, its single crystals were grown from this melt–solution using spontaneous nucleation followed by slow ((1–3)°C/day) cooling.

3. Crystallization and growth from the lithium-tungstate melt–solution

Another investigated solvent was lithium tungstate Li_2WO_4 used previously to grow trigonal rare-earth alumo-, scando-, and ferroborate single crystals. Growth from lithium-tungstate melt–solutions yielded crystals with the lowest contents of impurities of the melt–solution components [20].

Initially, a system similar to that used for alumo-, gallo-, and ferroborates was studied, which had a solvent component molar ratio of Li_2WO_4: B_2O_3: Tb_2O_3 = 1: 3.3: 0.3 and a stoichiometric crystal-forming oxide concentration (15 wt%). The temperature of nucleation in this melt–solution turned out to be 1090 °C. Fine terbium chromoborate crystals formed at the melt–solution surface and even finer Cr_2O_3 crystals, at the bottom of a crucible, which indicated insufficient homogeneity of the melt–solution. After repeated homogenization at a temperature of 1150 °C for 20 h using the same crystals, the saturation temperature was determined accurate to ± 5 °C, which was found to be (1115 ± 5)°C. In this case, the chromium oxide crystals completely dissolved.

The width $\Delta T_{met} \approx 12$ °C of the metastable region was determined as the maximum supercooling at which no nucleation of new single crystals occurred over a 20-h period. The regions of stability of terbium chromoborate crystals were found by direct phase probing.

The optimum composition of the melt–solution system in which terbium chromoborate was the only high-temperature phase can be written in the quasi-binary form.

$$85\ \text{wt}\ \%\ \{Li_2WO_4 + 3.3B_2O_3 + 0.3Tb_2O_3\} + 15\ \text{wt}\%\ TbCr_3(BO_3)_4 \quad (2)$$

Melt–solutions weighing 100 g were prepared at T = 1100 °C in a platinum cylindrical crucible (D = 60 mm, H = 65 mm) by fusing oxides [Li_2WO_4, B_2O_3, Tb_2O_3, and Cr_2O_3] in the ratio determined from formula (2). The crucible was installed in a crystallization furnace, in which the temperature was reduced from the bottom of the crucible with a vertical gradient of 1–2°C/cm. The melt–solution was first homogenized at T = 1100 °C for 24 h. To maintain the homogeneity, the melt–solution was mixed with a platinum rod rotating at a speed of 60 rpm. However, this appeared insufficient and the next homogenization at T = 1150 °C, also for 24 h, was performed. However, even after that, the melt–solution stayed inhomogeneous. Only after 24 h at a temperature of 1200 °C, homogeneity of the melt–solution was achieved.

To obtain $TbCr_3(BO_3)_4$ crystal seeds, the spontaneous nucleation technique was used again. To do this, after refining the saturation temperature and the metastability region width, a platinum rod was immersed in the melt–solution at the homogenization temperature and rotation at a speed of 40 rpm was switched on. After 2 h, the melt–solution temperature was reduced by 15 °C below the saturation temperature. The seeds were grown at a constant temperature for 24 h. Then, the rod was withdrawn from the furnace. The melt–solution residues were removed by boiling the rod in a 20 % aqueous solution of nitric acid. The grown seed crystals with predominantly trigonal symmetry were removed from the rod and used later to grow coarser crystals.

For this purpose, four visually high-quality seeds with a habit in the form of a hexagonal prism and an equilateral triangle at the top were fixed on a platinum rod holder. The holder was immersed into the melt–solution at a temperature of $T = T_{sat} + 7$ °C and reverse rotation at a speed of ω = 30 rpm with a period of 1 min was switched on. After 15 min, the temperature was reduced to $T = T_{sat} - 7$ °C. Then, the melt–solution temperature decreased at an increasing rate of 1–2°C per day, so that the crystal growth rate did not exceed 0.5 mm per day. The growth continued for 8 days. After completion of the growth process, the holder was raised above the melt–solution surface and cooled down to room temperature with the furnace power switched off. As a result, three single crystals up to 3 × 3 × 5 mm^3 in size with a habit characteristic of the trigonal phase were obtained.

The next stage was the spontaneous growth from the same melt–solution at a nucleation temperature lower by 10 and 15 °C than 1100 °C for 1–2 days. In this case, the monoclinic phase predominantly grew. No further growth of coarser monoclinic crystals using seeds was carried out; in the magnetic measurements, monoclinic single crystals obtained by spontaneous nucleation were used.

4. Characterization of the crystals

Fig. 1 presents photographs of typical single-crystal samples: (1) a trigonal single crystal grown from the lithium-tungstate melt–solution on a seed, (2) monoclinic single crystal synthesized from the same melt–solution, and (3) a monoclinic single crystal obtained from the bismuth molybdate melt–solution. The morphology of the crystals is mainly determined by their spatial symmetry. Trigonal crystal 1 grown from the lithium tungstate melt–solution on a seed has a shape characteristic of rare-earth Fe, Al, and Ga borates with the $\{11\bar{2}0\}$, $\{1\bar{2}10\}$and$\{2\bar{1}\bar{1}0\}$ side faces of a hexagonal prism and the $\{10\bar{1}1\}$, $\{0\bar{1}11\}$, and$\{\bar{1}101\}$ faces at the vertex. Such crystals often have a (0001) regular triangle perpendicular to the C_3 axis at the vertex.

Monoclinic crystals 2 and 3 grown using both melt–solutions also have the pronounced {0 1 0} and {1 1 1} faces of a hexagonal prism, but the faces at the vertex meet at a different angle than in the trigonal sample. Some monoclinic crystals have, in addition, triangular faces at

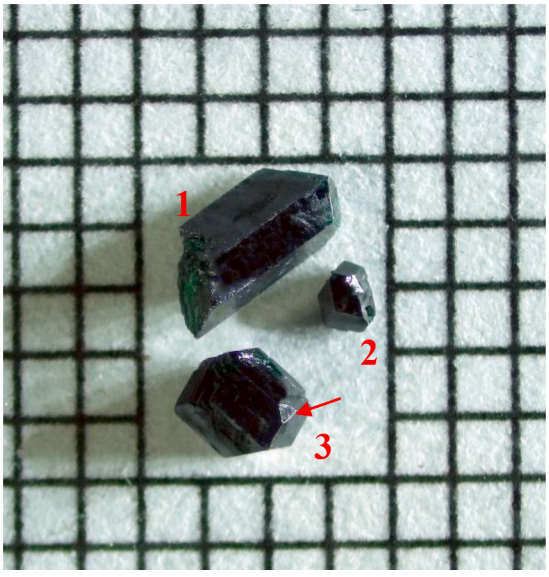

Fig. 1. Photograph of the synthesized $TbCr_3(BO_3)_4$ single crystals: (1) trigonal single crystal grown from the lithium-tungstate melt–solution on a seed, (2) monoclinic single crystal synthesized from the same melt–solution, and (3) monoclinic single crystal obtained from the bismuth-molybdate melt–solution. The grid step is 1 mm.

the vertex of a hexagonal prism that are perpendicular to its primary growth direction. Such a face in crystal 3 is indicated by the arrow in Fig. 1.

X-ray diffraction analysis of the structure of the grown single crystals was carried out using a Bruker AXS SMART APEX II single-crystal diffractometer and a Haoyuan DX-2700BH powder diffractometer at the Krasnoyarsk Regional Center for Collective Use, Krasnoyarsk Scientific Center, Siberian Branch of the Russian Academy of Sciences. X-ray powder diffraction patterns were obtained on the samples prepared by grinding of the single crystals. The measurements were performed on the crystals obtained using different solvents mentioned in this work.

As an example, Fig. 2 shows an X-ray powder diffraction pattern of the crystals obtained using bismuth trimolybdate $BiMo_3O_{12}$ as a solvent. The pattern corresponds to the monoclinic sp. gr. *C*2/*c*.

The X-ray diffraction study of the crystals grown using lithium tungstate Li_2WO_4 showed that, by varying the nucleation temperature of the single crystals, stable regions of the preferred growth of the trigonal or monoclinic phases of the terbium chromoborate single crystals can be found. It was established that the single crystals of both systems have similar habits. Therefore, to refine the structure and to control the crystallographic orientation of the samples for specific experimental investigations, additional methods were used, including the optical observations of conoscopic interference patterns in strongly converging light on a polarizing microscope and X-ray Lauegrams obtained on a Photonic Science Laue crystal orientation system.

To observe the conoscopic figures, two plates were made from the single crystals grown from the lithium-tungstate (Sample 1) and bismuth-molybdate (Sample 2) solvents. Both single crystals were subjected to preliminary magnetic testing. The habit of both single crystals is a hexagonal prism and the plates with a thickness of ~ 300 μM were cut perpendicular to its side faces. In this case, the plane of the plates is perpendicular to the single crystal growth direction. In polarized parallel light, these samples either exhibit optical anisotropy or not. Sample 2 uniformly fades and brightens upon rotation of the microscope stage with it, while Sample 1 only demonstrates local optical inhomogeneities in the form of light fading spots.

The conoscopic figure for Sample 1 (Fig. 3a) is a cross maintained upon rotation of the microscope stage (Fig. 3a'), which is characteristic of optically uniaxial crystals and is indicative of the trigonal symmetry. The cross is slightly deformed at its center due to the local optical inhomogeneity of the sample. The conoscopic figure for Sample 2 (Fig. 3b) is characteristic of the low-symmetry crystals: the emergence of two optical axes can be seen. As the microscope stage is rotated by 45° (Fig. 3b'), the conoscopic figure rotates as well and, due to the extinction, a dark stripe appears at the center. This figure is drastically different from the initial one observed at the diagonal position of the crystal (Fig. 3b). The aforesaid clearly evidences for the monoclinic symmetry of the crystal.

The crystal symmetry difference between Sample 1 and Sample 2 is confirmed by X-ray Lauegrams obtained by reflecting an X-ray beam oriented perpendicular to the plate plane. Figs. 4a and b present the Lauegrams for the trigonal and monoclinic $TbCr_3(BO_3)_4$ single crystals, respectively. The symmetry of reflections in the Lauegram shows that, in the trigonal crystal, the X-ray beam direction coincides with the C_3 axis, while the similar direction in the monoclinic crystal (the C_3 pseudo-axis) has a lower symmetry.

The lattice parameters determined using single-crystal and powder diffractometers are given in Table 1.

5. Magnetic properties

The magnetic properties of the obtained single crystals were measured on a PPMS-9 Physical Property Measurement System, which allows magnetic measurements in the temperature range of 2–300 K and magnetic fields of up to 90 kOe. The temperature dependences of the magnetization of the trigonal $TbCr_3(BO_3)_4$ single crystal, which was used to prepare Sample 1 for the conoscopic study, were measured in magnetic fields directed along the trigonal axis and in the basal plane. The measurement data are shown in Fig. 5; the inset to the figure presents the enlarged low-temperature portions of the curves.

It can be seen that, at both magnetic field directions, the temperature dependences of the magnetization contain two anomalies at temperatures of 5.5 and 9.2 K. The upper temperature is apparently the Néel temperature corresponding to the magnetic ordering of the Cr^{3+}

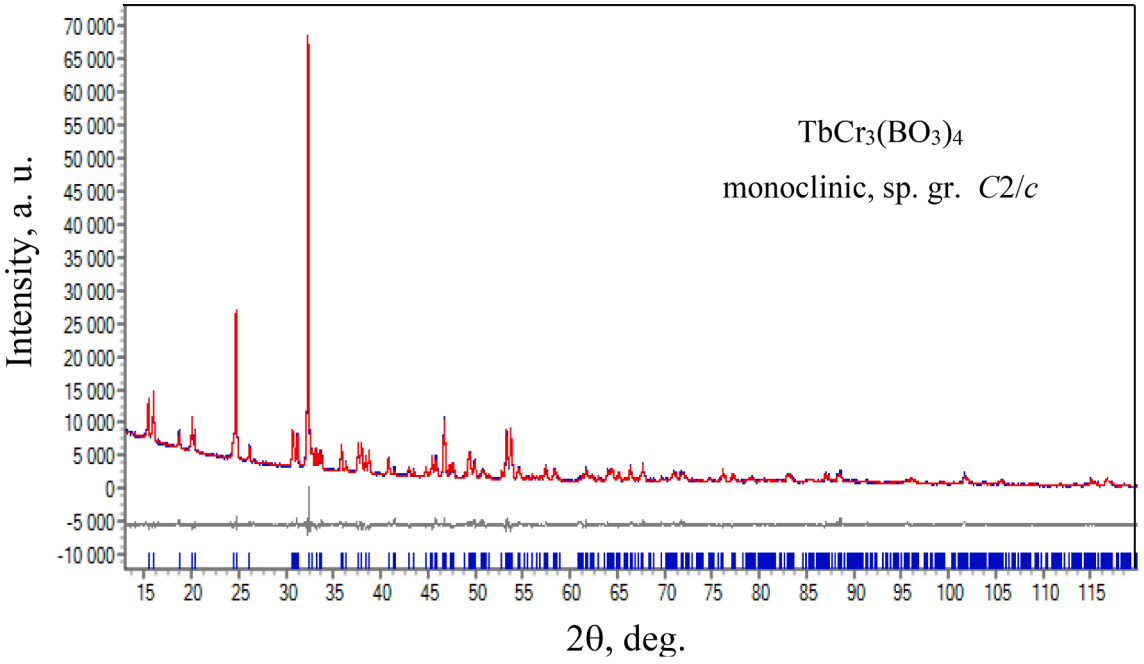

Fig. 2. X-ray powder diffraction pattern of the monoclinic crystals $TbCr_3(BO_3)_4$ obtained using bismuth-molybdate melt–solution. Comparison of the experimental (red line) and theoretical (blue line) spectra and difference between them (gray line). Vertical blue markers indicate the Bragg reflection positions. (For interpretation of the references to colour in this figure legend, the reader is referred to the web version of this article.)

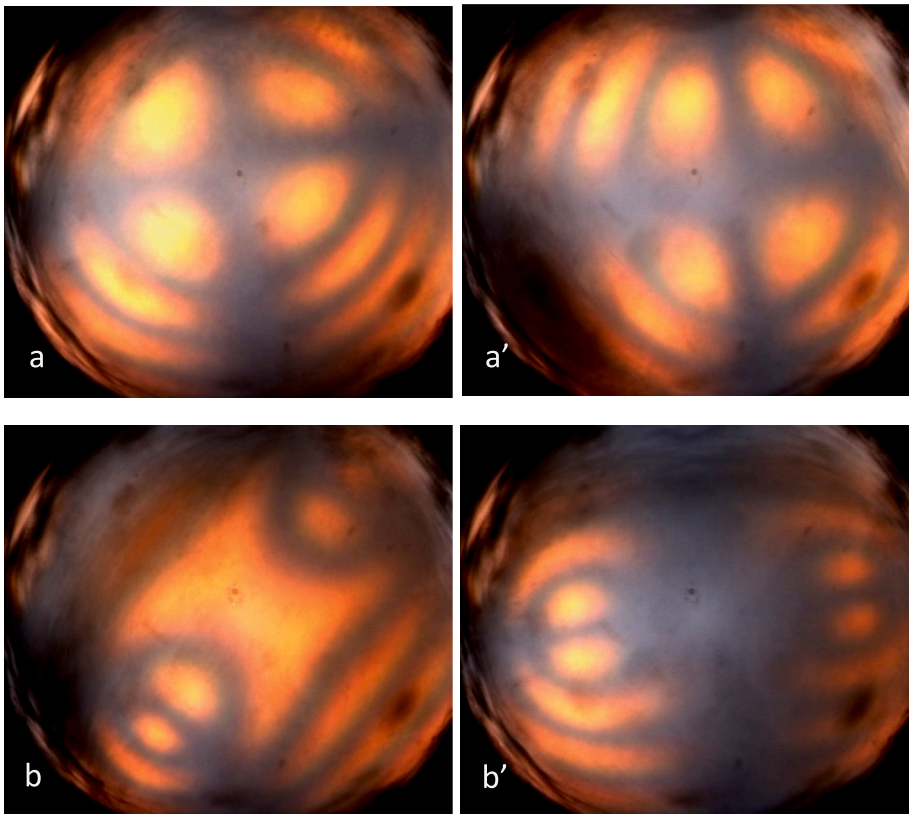

Fig. 3. Conoscopic figures for (a) trigonal Sample 1 and (b) monoclinic Sample 2 in their initial state and after rotating the microscope stage by 45° ((a') and (b'), respectively).

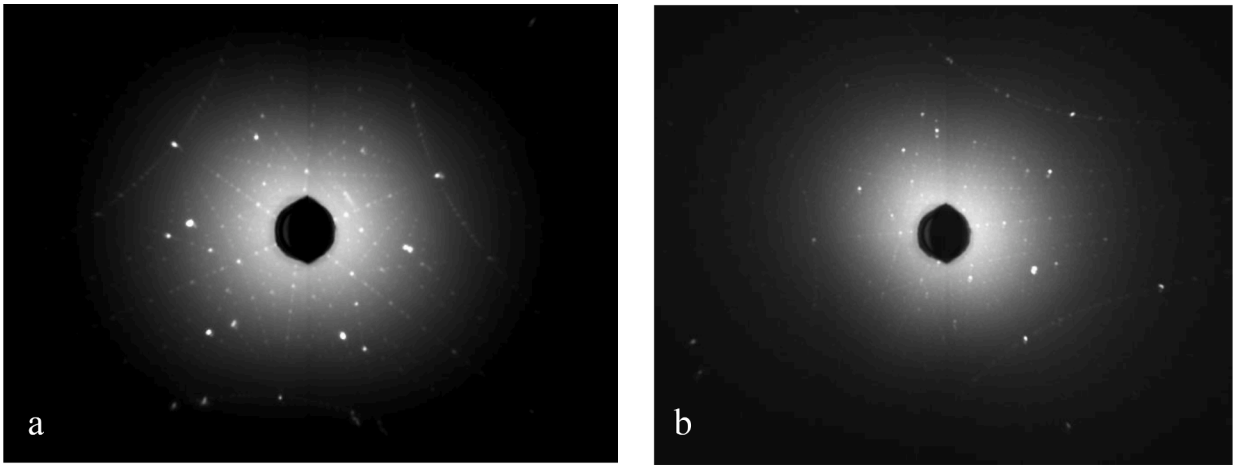

Fig. 4. X-ray Lauegrams for (a) the trigonal and (b) monoclinic $TbCr_3(BO_3)_4$ single crystal.

Table 1
Lattice parameters of the grown crystals.

Solvent	Symmetry	Lattice parameters, Å or °
Li_2WO_4:B_2O_3	R32	a = b = 9.4767(6), c = 7.4932(5)
Li_2WO_4:B_2O_3	C2/c	a = 7.4014(2); b = 9.4974(3), c = 11.4077(4), α= γ= 90, β = 103.845(1)
$Bi_2Mo_3O_{12}$: B_2O_3	C2/c	a = 7.3890(1); b = 9.4817(2), c = 11.3836(2), α= γ= 90, β = 103.812(1)

subsystem, while the lower-temperature anomaly most likely corresponds to the establishment of magnetic order in the Tb^{3+} ion subsystem. An abrupt drop of the magnetization below 5.5 K suggests that, in this temperature range, an antiferromagnetic structure with the easy anisotropy axis coinciding with the trigonal axis of the crystal is formed. At both magnetic field directions, $H||c$ and $H\perp c$, broad magnetization peaks are observed above the Néel temperature, which indicate the establishment of a short-range magnetic order.

The inset to the figure shows also the temperature dependence of the magnetization for the single crystal grown from the bismuth-molybdate melt–solution measured in the magnetic field $H||c$. It is this crystal that was later used to prepare Sample 2 for the conoscopic study. A

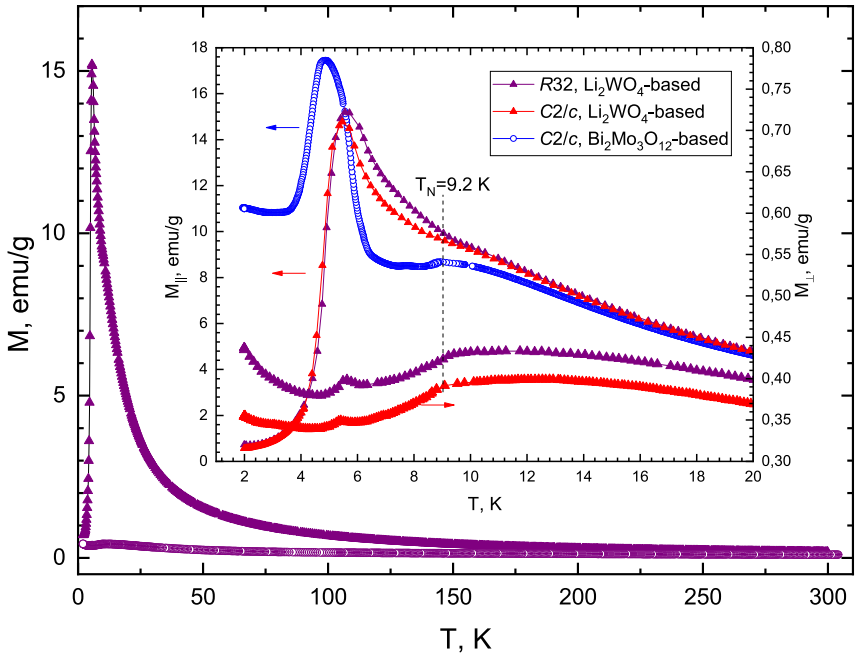

Fig. 5. Temperature dependences of the magnetization of the $TbCr_3(BO_3)_4$ single crystals synthesized from different solvents.

Fig. 5. Temperature dependences of the magnetization of the $TbCr_3(BO_3)_4$ single crystals synthesized from different solvents.

comparison with the data on the trigonal crystal shows that, in the paramagnetic region, the temperature dependences of the magnetization for both crystals are very similar, while in the low-temperature region they are drastically different. This difference could be caused by two reasons: different crystal structures of the samples or the effect of the Bi^{3+} impurity in the crystal grown from the bismuth-molybdate melt–solution. To elucidate the role of the crystal structure difference, the temperature dependences of the magnetization of a single crystal grown from the lithium-tungstate melt–solution at a lower nucleation temperature were measured. It was confirmed using the X-ray Lauegram that this single crystal has the monoclinic structure (sp. gr. *C*2/*c*). Based on the similarity of the habits of the trigonal and monoclinic crystals, which have the form of a hexagonal prism, the magnetic field orientation for the monoclinic crystal was also chosen relative to the preferred hexagonal prism growth axis: along the growth axis ($M_{||}$) and perpendicular to it ($M_{\perp}$). The temperature dependences of the magnetization of Sample 3 are also shown in the inset to Fig. 5. It can be seen that, at both field directions, the temperature dependences of the trigonal and monoclinic crystals are very similar over the entire measuring temperature range; minor differences at the perpendicular field direction are apparently due to the inaccuracy of the orientation of the sample relative to the magnetic field. Thus, it can be assumed that the main reason for the difference in the low-temperature behavior of the magnetization of the monoclinic $TbCr_3(BO_3)_4$ single crystals synthesized from the bismuth-molybdate melt–solution is the effect of the Bi^{3+} impurity, which partially replaces Tb^{3+} ions and leads to the distortions of oxygen environments of the neighboring ions.

A detailed experimental and theoretical description of the magnetic and thermodynamic properties of the obtained crystals and their magnetic phase diagram will be presented in a separate work.

6. Discussion

Possible causes for the formation of a structural modification in the huntite family crystals were studied in [21] by analyzing the structural properties and conditions for the synthesis of many rare-earth chromoborates $RCr_3(BO_3)_4$. The main structural modifications are the trigonal (sp. gr. *R*32 or $P312_1$) and monoclinic (sp. gr. *C*2 or *C*2/*c*) polytypes. Both of them are built from two different layers, L_{2n} and L_{2n+1}, which are identical for the two modifications. The L_{2n} layers contain pairs of edge-sharing MO_6 octahedra connected into a layer by isolated BO_3 triangles. The L_{2n+1} layers consist of RO_6 trigonal prisms and MO_6 octahedra connected in columns by vertices and also bound by BO_3 triangles. In the trigonal L_{2n+1} polytype, the layers with prisms multiply around the L_{2n} layers by two-fold axes, while in the monoclinic modification, they multiply by the symmetry centers.

Importantly, the trigonal and monoclinic modifications have very similar structures; therefore, it is difficult to establish exact temperature limits of the occurrence of the phases. The result obtained in [21] using the $K_2Mo_3O_{10}$-based solvent appeared opposite to that found by us: monoclinic $TbCr_3(BO_3)_4$ crystals were formed at higher crystallization temperatures (1040–1050 °C) and trigonal ones, at lower temperatures (900 – 950 °C). On the other hand, as was shown in [18], an increase in the percentage of the solvent in the growth charge and, correspondingly, an increase ~~a~~ in the crystallization temperature leads to an increase in the *R*32 phase content in the $TbCr_3(BO_3)_4$ crystals.

In [22], it was shown that the implementation of the trigonal or monoclinic polytype in the $RM_3(BO_3)_4$ (M = Fe, Al) crystals is governed by the ratio $r_{R^{3+}}/r_{M^{3+}}$ between the ionic radii. When this ratio exceeds a certain critical value, the trigonal polytype becomes unstable and passes to the monoclinic one. In the compounds with M = Cr, the critical ratio between the ionic radii is unknown, but it is obvious that this parameter in chromium borates also determines the implementation of a certain polytype. Then, the allowance for the impact of impurities becomes crucial. When the bismuth-molybdate melt–solution is used, bismuth ions partially replace rare-earth one. Since the Bi^{3+} ionic radius (1.03 Å) is larger than the Tb^{3+} one (0.92 Å), this partial substation increases the average radius $r_{R^{3+}}$ in the rare-earth site. It can be assumed that it is this process that stabilizes the monoclinic phase when the bismuth-molybdate melt–solution is used. Thus, the formation of a certain

$TbCr_3(BO_3)_4$ polytype also depends on the type of solvent, which can contaminate the crystals by impurity ions in different sites.

The impurity content in the lithium-tungstate melt–solution is much lower, which allows the existence of the trigonal phase. However, as the crystallization temperature lowers, the *C*2/*c* monoclinic phase can form.

7. Conclusions

Crystallization of terbium chromoborate $TbCr_3(BO_3)_4$ single crystals in two different melt–solution systems based on bismuth trimolybdate $Bi_2Mo_3O_{12}$ and lithium tungstate Li_2WO_4 was studied. The regions of stability of the crystals were determined by direct phase probing. It was shown that, in the bismuth trimolybdate-based melt–solutions with all the investigated solvent component ratios and crystal-forming oxide concentrations, only the terbium chromoborate monoclinic phase with sp. gr. *C*2/*c* crystallizes.

In the lithium tungstate-based melt–solutions, the solvent component ratio was determined at which, above 1100 °C, the terbium chromoborate trigonal phase with sp. gr. *R*32 mainly crystallizes. Below this temperature, the monoclinic phase *C*2/*c* dominates. It was assumed that the stabilization of the monoclinic phase when using the bismuth-molybdate melt–solution can be caused by an increase in the average ionic radius in the rare-earth ion site under partial substitution of bismuth ions for terbium ones.

The X-ray diffraction and conoscopic investigations proved the possibility of obtaining two structural modifications of terbium chromium borate. The lattice parameters of the crystals grown from different melt–solutions were refined.

The magnetic characteristics of the grown single crystals were measured. It was shown that the difference in the behavior of the magnetic properties of the monoclinic phase crystals grown from different melt–solutions is most likely due to the partial inclusion of bismuth ions instead of terbium ions in the crystals grown from the bismuth trimolybdate solvent. At the same time, the structural differences between the crystals do not affect their magnetic properties: the temperature dependences of the magnetization of the monoclinic and trigonal crystals synthesized from the lithium tungstate solvent were found to be very similar.

It was suggested that the first of the noted anomalies in the temperature dependence ($T_{N1} = 9.2$ K) is the Néel temperature of the subsystem of chromium ions and the second one ($T_{N2} = 5.5$ K) is caused by magnetic ordering of the terbium subsystem.

CRediT authorship contribution statement

I.A. Gudim: Writing – review & editing, Writing – original draft, Validation, Supervision, Resources, Investigation, Funding acquisition, Data curation, Conceptualization. **N.V. Mikhashenok:** Writing – original draft, Validation, Supervision, Investigation. **A.D. Vasiliev:** Validation, Investigation, Data curation. **S.V. Melnikova:** Validation, Investigation, Data curation. **M.S. Pavlovskii:** Validation, Investigation, Formal analysis, Data curation. **S.A. Skorobogatov:** Validation, Formal analysis, Data curation. **A.I. Pankrats:** Writing – review & editing, Writing – original draft, Validation, Supervision, Investigation, Data curation, Conceptualization.

Declaration of competing interest

The authors declare that they have no known competing financial interests or personal relationships that could have appeared to influence the work reported in this paper.

Data availability

No data was used for the research described in the article.

Acknowledgments

The authors thank A.V. Zamkov for assistance in preparing the samples for the conoscopic study. The characterization and examination of the samples were performed at the Center for Collective Use, Krasnoyarsk Scientific Center, Siberian Branch of the Russian Academy of Sciences.

Funding

This study was supported in part by the Russian Science Foundation and the Krasnoyarsk Territorial Foundation for Support of Scientific and R&D Activity, project no. 22-12-20019.

References

[1] K.-C. Liang, R.P. Chaudhury, B. Lorenz, Y.Y. Sun, L.N. Bezmaternykh, V. L. Temerov, C.W. Chu, Phys. Rev. B 83 (2011) 180417.
[2] T. Usui, Y. Tanaka, H. Nakajima, M. Taguchi, A. Chainani, M. Oura, S. Shin, N. Katayama, H. Sawa, Y. Wakabayashi, T. Kimura, Nat. Mater. 13 (2014) 611.
[3] Ph. Goldner, O. Guillot-Noël, J. Petit, M. Popova, L. Bezmaternykh, Phys. Rev. B 76 (2007) 165102.
[4] J. Liao, Y. Lin, Y. Chen, Z. Luo, Y. Huang, J. Cryst. Growth 267 (2004) 134–139.
[5] L.M. Dorozhkin, I.I. Kurstev, N.I. Leonyuk, T.I. Rimchenko, A.V. Shestakov, Sov. Thech. Phys. Lett. 7 (1981) 555–556.
[6] Tu. Chaoyang, Z. Zhu, J. Li, Y. Huang, Wu. Baichang, M. Huang, Z. Chen, Opt. Mater. 27 (2004) 167–171.
[7] Ran He, Lin Z. S., Lee M.-H., and Chen C. T. // Journal of Applied Physics 109, 2011, 103510.
[8] Ch. Tu, M. Qiu, Y. Huang, X. Chen, A. Jiang, Z. Luo, J. Cryst. Growth 208 (2000) 487–492.
[9] E.A. Popova, D.V. Volkov, A.N. Vasiliev, A.A. Demidov, N.P. Kolmakova, I. A. Gudim, L.N. Bezmaternykh, N. Tristan, Yu. Skourski, B. Buechner, C. Hess, R. Klingeler, Phys. Rev. B 75 (2007) 224413.
[10] D.V. Volkov, E.A. Popova, N.P. Kolmakova, A.A. Demidov, N. Tristan, Yu. Skourski, B. Buechner, I.A. Gudim, L.N. Bezmaternykh, JMMM 316 (2007) e717–e720.
[11] Zvezdin A.K., Vorob'ev G.P., Kadomtseva A.M., Popov Yu.F., Pyatakov A.P., Bezmaternykh L.N., Kuvardin A.V. and Popova E.A. // JETP Letters, 83, 2006, 509-514.
[12] A.S. Aleksandrovsky, I.A. Gudim, A.S. Krylov, V.L. Temerov, Phys. Solid State 49 (9) (2007) 1695–1699.
[13] N.V. Volkov, I.A. Gudim, E.V. Eremin, A.I. Begunov, A.A. Demidov, K.N. Boldyrev, JETP Lett. 99 (2014) 67–75.
[14] Eremin E.V., Pavlovskiy M.S., Gudim I.A., Temerov V., Molokeev M., Andryushin N.D., Bogdanov E.V. // Journal of Alloys and Compounds 828, 2020, 154355.
[15] Wang G.F. in: Wu X.T., Chen L. (Eds.), Structure-Property Relationships in Nonlinear Optical Crystals I. Structure and Bonding, vol. 144, Springer, Berlin, 2012, 105-120.
[16] N.I. Leonyuk, V.V. Maltsev, E.A. Volkova, O.V. Pilipenko, E.V. Koporulina, V. E. Kisel, N.A. Tolstik, S.V. Kurilchik, N.V. Kuleshov, Opt. Mater. 30 (1) (2007) 161–163.
[17] Xu. Yongyuan, X. Gong, Y. Chen, M. Huang, Z. Luo, Y. Huang, J. Cryst. Growth 252 (2003) 241–245.
[18] N.N. Kuzmin, V.V. Maltsev, E.A. Volkova, N.I. Leonyuk, K.N. Boldyrev, A. N. Bludov, Inorg. Mater. 56 (8) (2020) 828–835.
[19] K.N. Boldyrev, M.N. Popova, M. Bettinelli, V.L. Temerov, I.A. Gudim, L. N. Bezmaternykh, P. Loiseau, G. Aka, N.I. Leonyuk, Opt. Mater. 34 (2012) 1885–1889.
[20] Eremin E.V., Pavlovskiy M.S., Gudim I.A., Temerov V., Molokeev M., Andryushin N.D., Bogdanov E.V. // Journal Of Alloys And Compounds 828, 2020, 154355.
[21] Borovikova E.Yu., Dobretsova E.A., Boldyrev K.N., Kurazhkovskaya V.S. Maltseva V.V, Leonyuk N.I. // Vibrational Spectroscopy, 68, 2013, 82.
[22] N.I. Leonyuk, L.I. Leonyuk, Prog. Cryst. Growth Charact. 31 (1995) 179.